

HOT ORGANIC MOLECULES TOWARD A YOUNG LOW-MASS STAR: A LOOK AT INNER DISK CHEMISTRY

F. LAHUIS^{1,2}, E.F. VAN DISHOCK¹, A.C.A. BOOGERT³, K.M. PONTOPPIDAN^{1,4}, G.A. BLAKE⁴, C.P. DULLEMOND⁵, N.J. EVANS II⁶,
M.R. HOGERHEIJDE¹, J.K. JØRGENSEN⁷, J.E. KESSLER-SILACCI⁶, AND C. KNEZ⁶

Draft version October 14, 2019

ABSTRACT

Spitzer Space Telescope spectra of the low mass young stellar object (YSO) IRS 46 ($L_{\text{bol}} \approx 0.6 L_{\odot}$) in Ophiuchus reveal strong vibration-rotation absorption bands of gaseous C_2H_2 , HCN, and CO_2 . This is the only source out of a sample of ~ 100 YSO's that shows these features and the first time they are seen in the spectrum of a solar-mass YSO. Analysis of the Spitzer data combined with Keck L - and M -band spectra gives excitation temperatures of $\gtrsim 350$ K and abundances of $10^{-6} - 10^{-5}$ with respect to H_2 , orders of magnitude higher than those found in cold clouds. In spite of this high abundance, the HCN $J = 4 - 3$ line is barely detected with the James Clerk Maxwell Telescope, indicating a source diameter less than 13 AU. The (sub)millimeter continuum emission and the absence of scattered light in near-infrared images limits the mass and temperature of any remnant collapse envelope to less than $0.01 M_{\odot}$ and 100 K, respectively. This excludes a hot-core type region as found in high-mass YSO's. The most plausible origin of this hot gas rich in organic molecules is in the inner (< 6 AU radius) region of the disk around IRS 46, either the disk itself or a disk wind. A nearly edge-on 2-D disk model fits the spectral energy distribution (SED) and gives a column of dense warm gas along the line of sight that is consistent with the absorption data. These data illustrate the unique potential of high-resolution infrared spectroscopy to probe organic chemistry, gas temperatures and kinematics in the planet-forming zones close to a young star.

Subject headings: infrared: ISM – ISM: individual (IRS 46) – ISM: jets and outflows – ISM: molecules – planetary system: protoplanetary disks – stars: formation

1. INTRODUCTION

The presence of gas-rich disks around young stars is well established observationally and theoretically (see review by Greaves 2005), but comparatively little is known about their chemical structure. A good understanding of the chemistry is important since part of the gases and solids in protoplanetary disks will end up in future solar systems where they may form the basis for prebiotic species (see reviews by Ehrenfreund & Charnley 2000; Markwick & Charnley 2004). Virtually all observational studies of molecules other than CO have been limited to the outer regions, where simple organic molecules such as HCO^+ , CN, HCN, and H_2CO have been detected at millimeter wavelengths (e.g. Dutrey, Guilloteau & Guélin 1997; Kastner et al. 1997; Qi et al. 2003; Thi, van Zadelhoff & van Dishoeck 2004). Because of beam dilution, these observations cannot probe radii < 50 AU from the star, which is the relevant zone for planet formation. High-resolution infrared (IR) spectroscopy has found CO emission from the warm dense gas in the inner disk region (Najita, Carr & Mathieu 2003; Brittain et al. 2003; Blake & Boogert 2004), but H_2O is the only molecule besides CO and H_2 which has been convincingly detected (Carr, Tokunaga & Najita 2004).

Models of inner disk chemistry initially focused on our own

primitive solar nebula (see review by Prinn 1993) but now also consider exosolar systems. They have grown considerably in sophistication, including non-equilibrium chemistry, gas-solid interactions, radial and vertical mixing, and the effects of UV radiation and X-rays from the central star on the gas temperature and molecular abundances (e.g., Markwick et al. 2002; Gail 2002; Ilgner et al. 2004; Glassgold, Najita & Igea 2004; Gorti & Hollenbach 2004). Large abundances of organic molecules like C_2H_2 and HCN are predicted in some of these models in the inner few AU, but no observational tests have been possible to date.

The sensitive Infrared Spectrograph (IRS) on board the Spitzer Space Telescope opens a new window to study molecules in disks through IR pencil-beam line-of-sight absorption spectroscopy. The Spitzer c2d legacy program “From Molecular Cores to Planet-Forming Disks” (Evans et al. 2003) is collecting a coherent sample of IRS spectra of low-mass YSO's in five nearby star-forming regions. To date more than 100 Class I and Class II sources have been observed. Of these only one source, IRS 46, shows strong gas-phase absorption bands of hot molecules. These gas-phase bands have previously been seen only toward deeply embedded high-mass YSO's, where they have been associated with the inner ($\lesssim 1000$ AU) warm dense regions of the spherical envelopes, also known as ‘hot cores’ (Carr et al. 1995; Lahuis & van Dishoeck 2000; Boonman et al. 2003). The sources studied with Spitzer have factors of $10^4 - 10^5$ lower luminosity, thus limiting the maximum temperatures and amount of warm gas in the envelope.

IRS 46, also known as YLW16b and GY274, is part of the Ophiuchus cloud at a distance of ~ 125 pc (de Geus, de Zeeuw & Lub 1989). It is classified as a Class I source, i.e., a protostar with a compact accretion disk embedded in a more extended and collapsing envelope, based on its near- and mid-IR colors (André & Montmerle 1994) with

¹ Leiden Observatory, P.O. Box 9513, 2300 RA Leiden, The Netherlands

² SRON Netherlands Institute for Space Research, P.O. Box 800, 9700 AV Groningen, The Netherlands
Electronic address: F.Lahuis@sron.rug.nl

³ Division of PMA, MS 105-24, Caltech, Pasadena, CA 91125, USA

⁴ Division of GPS, MS 150-21, Caltech, Pasadena, CA 91125, USA

⁵ Max-Planck-Institut für Astronomie, Königstuhl 17, D-69117 Heidelberg, Germany

⁶ Department of Astronomy, University of Texas at Austin, 1 University Station C1400, Austin, TX 78712-0259

⁷ Harvard-Smithsonian Center for Astrophysics, 60 Garden Street, Mail Stop 42, Cambridge, MA 02138, USA

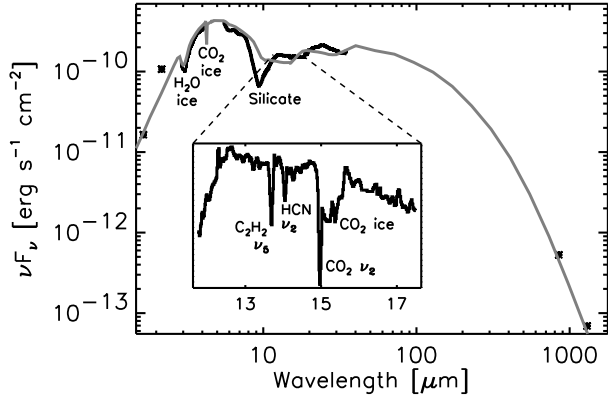


FIG. 1.— Composite SED of IRS 46 from 1.25 μm to 1.3 mm including the full Spitzer IRS spectrum from 10–37 μm , 2MASS J, H, K_s imaging and photometry ($F_J = 0.33$ mJy, $F_H = 9.03$ mJy, $F_{K_s} = 77.5$ mJy), a VLT-ISAAC L -band spectrum at $R \approx 1200$ (Pontoppidan et al. 2003), an ISOCAM-CVF 5–16 μm spectrum at $R \approx 50$, $F_{850 \mu\text{m}} = 150$ mJy (see Ridge et al. 2006), and $F_{1.3 \text{ mm}} = 28$ mJy (André & Montmerle 1994). Overplotted in grey is a SED disk model of a nearby edge-on self-shadowed flaring disk of 60 AU radius with $L_{\text{bol}} \approx 0.6 L_{\odot}$ and a disk mass of $\sim 0.03 M_{\odot}$ seen at an inclination of $\sim 75^\circ$. The insert shows a zoom-in on the mid-IR region showing the observed C_2H_2 , HCN, and CO_2 molecular absorption features and the CO_2 ice band at 15 μm .

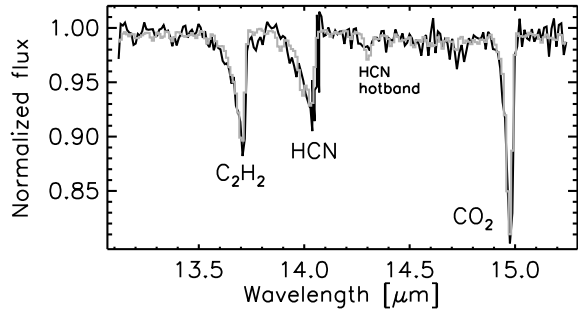


FIG. 2.— Blow-up of the IRS 46 normalized Spitzer-IRS spectrum covering the $\text{C}_2\text{H}_2 \nu_5 = 1-0$, $\text{HCN} \nu_2 = 1-0$, and $\text{CO}_2 \nu_2 = 1-0$ bending mode ro-vibrational absorption bands. Included in grey is a best fit synthetic spectrum.

$L_{\text{bol}} \approx 0.6 L_{\odot}$ (Bontemps et al. 2001). However, the complete SED is also consistent with a Class II source viewed nearly edge-on, i.e., a pre-main sequence star with a disk but without a significant collapse envelope (see Sect. 4). It is similar to the SED of the nearby edge-on disk CRBR 2422.8-3423 (Pontoppidan et al. 2005), but IRS 46 has less dense foreground material. The favorable inclination of CRBR 2422.8-3423 allows for the study of ices in the outer region of the circumstellar disk. IRS 46, also profiting from a favorable inclination, may prove to offer a unique opportunity to directly study the gas temperature and hot gas-phase organic chemistry in the inner disk.

2. OBSERVATIONS

IRS 46 was observed with Spitzer-IRS in the SH (9.9–19.6 μm) and LH (18.7–37.2 μm) medium-resolution modes. The observation was positioned at $16^{\text{h}}27^{\text{m}}29^{\text{s}}.4 - 24^{\circ}39'16''.3$ (J2000) and acquired on 2004 August 29 as part of AOR# 0009829888. Low resolution SL and LL observations are scheduled as part of the Spitzer GTO program but have not yet been taken. Data reduction started from the BCD images using S11.0.2 Spitzer archive data. The processing includes

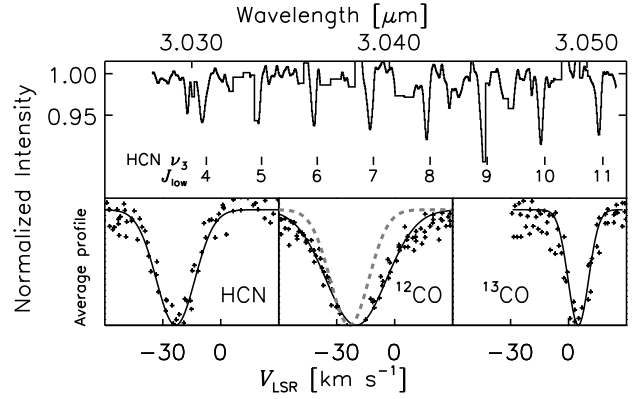


FIG. 3.— Top: Keck-NIRSPEC L -band spectrum showing HCN ν_3 C-H stretching mode absorption lines with tickmarks at the rest wavelengths. Bottom: HCN and CO velocity components derived from Keck-NIRSPEC L - and M -band spectra using absorption lines with an atmospheric transmission $> 40\%$. Plus symbols show the observed data, solid lines the fitted Gaussian velocity profiles. In the ^{12}CO profile plot the HCN profile is included (dashed grey line) showing that the HCN and CO lines are blue-shifted by a similar amount but that the CO profile is broader.

bad-pixel correction, extraction, defringing, and order matching using the c2d analysis pipeline (Lahuis, in preparation; Kessler-Silacci et al. 2005).

Figure 1 shows the SED composed from the full Spitzer-IRS spectrum and complementary archival and literature data. Figure 2 shows the part of the (normalized) IRS spectrum revealing the $\text{C}_2\text{H}_2 \nu_5 = 1-0$, $\text{HCN} \nu_2 = 1-0$, and $\text{CO}_2 \nu_2 = 1-0$ bending mode ro-vibrational absorption bands. Included is a best-fit synthetic spectrum (see Section 3).

To constrain the source size of the warm gas, JCMT⁸ HCN $J = 4-3$ and CO $J = 3-2$ spectra at 354 GHz and 345 GHz were obtained using receiver B3. A weak HCN line with $T_{\text{MB}} = 0.035$ K and $\Delta V \approx 6 \text{ km s}^{-1}$ at $V_{\text{LSR}} = 4.4 \text{ km s}^{-1}$ is detected. The CO $J = 3-2$ line is strong, $T_{\text{MB}} \approx 10$ K at the same velocity. A small CO map around IRS 46 reveals only a red wing, most likely associated with the outflow from IRS 44.

High-resolution L - and M -band spectra ($R \approx 25,000$) were obtained with the NIRSPEC spectrometer at the Keck II telescope⁹ to provide kinematic information and confirmation of the Spitzer HCN detection through the CO $\nu = 1-0$ 4.7 μm and HCN $\nu_3 = 1-0$ 3.0 μm stretching mode ro-vibrational bands (see Figure 3). The ^{13}CO absorption lines are unresolved at the quiescent cloud velocity of $V_{\text{LSR}} \approx 4 \text{ km s}^{-1}$. However, the resolved ^{12}CO ($\Delta V \approx 30 \text{ km s}^{-1}$) and HCN ($\Delta V \approx 20 \text{ km s}^{-1}$) absorption lines are observed to be shifted, at $V_{\text{LSR}} \approx -20 \text{ km s}^{-1}$. Of these no counterpart is observed in the HCN $J = 4-3$ and CO $J = 3-2$ JCMT spectra. We associate the HCN, C_2H_2 , and CO_2 absorptions seen in the Spitzer spectra with the blue-shifted components.

3. ANALYSIS

The Spitzer spectra are analyzed using a pure absorption model assuming local thermodynamic equilibrium (LTE) excitation of the levels at a single temperature. The adopted method is described in detail in Lahuis & van Dishoeck (2000) and Boonman et al. (2003), which includes references to the molecular parameters and data used in the model. The main fit parameters are the average temperature and integrated

⁸ The JCMT is operated by the JAC in Hilo, Hawaii on behalf of PPARC (UK), NRC (Canada) and NWO (Netherlands)

⁹ The W.M. Keck Observatory is operated as a scientific partnership among Caltech, the University of California and NASA, made possible by the W.M. Keck Foundation

column density along the line of sight for a given intrinsic line width, defined by the Doppler b -value. The resolved HCN ν_3 lines can be the result of multiple unresolved components along the line of sight, so that the intrinsic b value can be smaller than the observed line width. For small b -values $< 2 \text{ km s}^{-1}$, no good fit can be made to the $\text{C}_2\text{H}_2 \nu_5$ and $\text{CO}_2 \nu_2$ profiles. Therefore, b is taken to range from 2 to 12 km s^{-1} .

The best fits to the $\text{C}_2\text{H}_2 \nu_5$, HCN ν_2 , and $\text{CO}_2 \nu_2$ bands observed in the IRS spectrum give T_{ex} of ~ 700 , 400, and 300 K and column densities of 3, 5, and $10 \times 10^{16} \text{ cm}^{-2}$ respectively for $b \approx 5 \text{ km s}^{-1}$. The uncertainty in b results in an uncertainty of 25% in these values. The blue-shifted CO $\nu = 1-0$ absorption band gives $T_{\text{ex}} = 400 \pm 100 \text{ K}$ and $N = (2 \pm 1) \times 10^{18} \text{ cm}^{-2}$ corresponding to a minimum H_2 column density of $1 \times 10^{22} \text{ cm}^{-2}$ assuming a CO abundance of 2×10^{-4} (all gas-phase carbon in CO), as appropriate for warm dense gas. The $9.7 \mu\text{m}$ silicate depth corresponds to $N_{\text{H}} = 3 \times 10^{22} \text{ cm}^{-2}$ assuming a conversion factor: $N_{\text{H}} = \tau_{9.7} \times 3.5 \times 10^{22} \text{ cm}^{-2}$ (see Draine 2003). X-ray observations give $N_{\text{H}} = 11(\pm 7) \times 10^{22} \text{ cm}^{-2}$ (Imanishi, Koyama & Tsuboi 2001). Assuming most hydrogen is in H_2 and allowing for some foreground absorption in the latter two determinations, all estimates are consistent with $N(\text{H}_2) = 1 \times 10^{22} \text{ cm}^{-2}$ within a factor of two. The resulting abundance estimates are 3, 5, and 10×10^{-6} for C_2H_2 , HCN, and CO_2 , respectively. The density of the gas is at least 10^8 cm^{-3} , required to thermalize HCN and C_2H_2 .

Additional constraints can be obtained from a combined analysis of the HCN ν_2 and ν_3 bands (Figure 3). Assuming the same excitation temperature for both bands, the required column density to fit the ν_3 band is higher by a factor of 4 than that found from the ν_2 band. This suggests that geometrical effects and emission filling in the absorption may play an important role (see Boonman et al. 2003). One possibility is that the absorbing region is smaller than the continuum emitting region, the size of which may depend on wavelength. Similar increases may be expected for C_2H_2 and CO_2 . Thus, the above cited abundances are lower limits. The inferred HCN abundance, with respect to both H_2 and CO, is up to four orders of magnitude larger than that found in cold interstellar clouds.

4. DISCUSSION

Where does this hot gas rich in organic molecules reside? The first clue comes from the HCN submillimeter JCMT spectrum. For a HCN column density of $> 10^{17} \text{ cm}^{-2}$ derived from the IR data, the $J=4-3$ pure rotational line is highly optically thick. Thus, T_{MB} is expected to be close to the excitation temperature of $\sim 400 \text{ K}$ if the emission would fill the beam. Although a weak emission line is observed at $V_{\text{LSR}} \approx 4 \text{ km s}^{-1}$, the broad -20 km s^{-1} component is not detected with a 3σ limit of 0.02 K in a 1 km s^{-1} bin. This gives a beam dilution $\gtrsim 2 \times 10^4$ which, for the JCMT beam size of $15''$, implies a source diameter for the hot gas of $\lesssim 0.11''$ or 13 AU diameter at the distance of Ophiuchus. A similar limit follows from the lack of a blue wing on the CO $J=3-2$ line.

The second clue comes from the high temperatures and densities of the molecular gas. In general, temperatures of a few hundred K are found in YSO environments only in the innermost part of envelopes or in the inner disks. The velocity of the hot gas provides a final clue. The radial velocity of IRS 46 is unknown, and it is possible that IRS 46 itself is at a velocity of -20 km s^{-1} (Doppmann et al. 2005). More likely, however, IRS 46 is close to the nominal cloud velocity of 4.4 km s^{-1} and

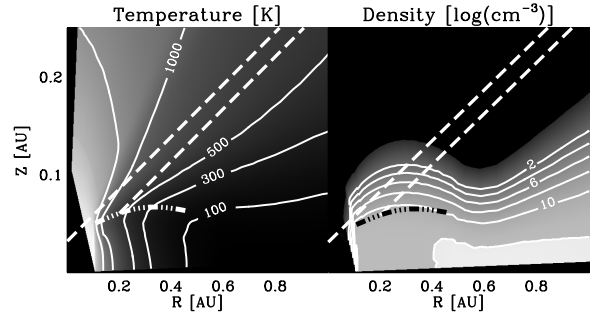


FIG. 4.— 2-D distribution of the temperature (left) and density (right) in the inner disk for the best-fitting model to the SED. Included are the $\tau = 1$ photosphere at $14 \mu\text{m}$ (dot-dashed curves) and two lines of sight (dashed lines) at the disk inclination of 75° . Most of the molecular absorption originates along the lines of sight toward the photosphere in the hot ($> 300 \text{ K}$) inner rim and toward the hot surface (1500 K) of the inner rim on the opposite side of the star (see Section 4).

the hot gas is blue-shifted by $\sim 25 \text{ km s}^{-1}$.

Based on these arguments, three possibilities are considered for the location of this hot gas: (i) the inner layer of any remnant collapse envelope on scales $\lesssim 100 \text{ AU}$ around IRS 46; (ii) the inner $\lesssim 10 \text{ AU}$ regions of a nearly edge-on disk; and (iii) dense hot gas at the footpoint of a wind launched from the inner disk. The first two options are examined through radiative transfer models to constrain the physical parameters of the source environment.

To explore the first option, a spherically symmetric model with a power-law density distribution was constructed reproducing the SCUBA submillimeter continuum map and the SED of IRS 46 from mid-IR to submillimeter wavelengths following Jørgensen, Schöier & van Dishoeck (2002). This model has two severe problems: to reproduce the mid-IR continuum emission, the temperature in the innermost envelope cannot exceed roughly 100 K; and a $\sim 0.01 M_\odot$ envelope (estimated from the submillimeter continuum data) produces a significant scattering nebulosity at near IR wavelengths which is not observed in VLT-ISAAC images (Pontoppidan et al. 2005). The envelope model also cannot explain the line widths and velocities unless IRS 46 itself is at -20 km s^{-1} . Thus, most of the IR and submillimeter continuum emission must arise from the disk around IRS 46.

To investigate the second option, the physical structure of the IRS 46 disk was constrained from the observed SED in a manner similar to CRBR 2422.8-3423 (Pontoppidan et al. 2005) using the 2-D axisymmetric Monte Carlo radiative transfer code of Dullemond & Dominik (2004). Figure 4 shows the temperature and density structure of the hot inner part of the nearly edge-on self-shadowed flaring disk and Figure 1 the best fitting SED. There is some degeneracy in the parameters of the best-fitting model (see the discussion in Pontoppidan et al. 2005), but spatially resolved data are needed to further constrain the fits. The fit to the silicate feature is sensitive to the assumed opacities, emission from the outer disk, and the presence of foreground absorption; these uncertainties have little impact on the part of the disk model relevant to this work, i.e., the dense inner disk region.

The main continuum contribution from the disk at $3-14 \mu\text{m}$ comes from the puffed up inner rim and inner rim wall on the far side of the star. In the disk model, the integrated column of dense gas ($> 10^8 \text{ cm}^{-3}$) toward these areas ranges from $1-2 \times 10^{22} \text{ cm}^{-2}$ with average temperatures of 300–1500 K. This is consistent with the H_2 column density and temperatures derived from the observations (see Section 3). Indeed,

more generally, the observed temperatures are consistent with disk models which explicitly calculate the gas temperature in the inner disk. The gas temperatures may be even higher than the dust temperatures in the upper layers (Glassgold et al. 2004; Gorti & Hollenbach 2004). The velocity broadened CO and HCN profiles (Figure 3) could result from absorption in the Keplerian inner rim at 0.1 AU ($V_{\text{kep}} \approx 70 \text{ km s}^{-1}$ for a $0.5 M_{\odot}$ star). If IRS 46 is at the cloud velocity of $+4 \text{ km s}^{-1}$, the blue-shifted absorption implies a deviation from Keplerian rotation in the disk plane, for example as the result of a close binary. A near edge-on disk explanation is consistent with a detection toward only one in a hundred objects, since a very small fraction of sources should have the right orientation.

A blue-shifted velocity may also indicate that the observed absorption features originate in a wind emanating from the inner disk. Possibilities include a magnetocentrifugal wind (either an X-wind launched within 0.1 AU or a disk wind launched further out), a photoevaporative flow or stellar wind interacting with the upper layer and entraining molecular material (see e.g. Eisloffel et al. 2000). For the gas to be seen in absorption it must be comparable in size to the inner disk region responsible for the $14 \mu\text{m}$ background, i.e. a few AU in radius. For a smaller region the background continuum will dominate whereas for a much larger region line emission from the warm molecular gas will fill in or dominate the absorption. For a few AU region, the mass loss rate would be of order $10^{-7} - 10^{-6} M_{\odot} \text{ yr}^{-1}$ assuming a density of $\geq 10^8 \text{ cm}^{-3}$, a total H_2 column of 10^{22} cm^{-2} , and a flow velocity of $\sim 25 \text{ km s}^{-1}$. IRS 46 does not show strong accretion signatures so a higher flow rate seems unlikely. Quantitative predictions in terms of velocities, column densities, densities and temperatures of the molecular gas are needed to distinguish between the above models.

Regardless of the precise origin in the disk or disk wind, the high inferred excitation temperatures of 400–900 K and high abundances of HCN and C_2H_2 of $10^{-6} - 10^{-5}$ are characteristic of high temperature chemistry. Hot chemistry in general is dominated by evaporation of the molecules from the grains with subsequent gas-phase processing. At high temperatures,

the hydrocarbon and nitrogen chemistry are enhanced as most of the oxygen is converted into water by neutral-neutral reactions. The abundances of molecules such as C_2H_2 , CH_4 , and HCN can be increased by orders of magnitude (e.g. Doty et al. 2002; Rodgers & Charnley 2003) while at the same time the formation of CO_2 is reduced as its primary formation route through OH is blocked. Interestingly, CO_2 has a lower excitation temperature in our observations. The most recent models of inner disk chemistry predict enhanced abundances of HCN and C_2H_2 . In particular, Markwick et al. (2002) give HCN, C_2H_2 , and CO_2 abundances of $10^{-6} \sim 10^{-5}$ in the inner 1 AU of a protoplanetary disk, in good agreement with the abundances found in this work.

In summary, we present the first detection of gaseous molecular absorption bands with Spitzer toward a solar-mass YSO, which offer direct, unique probes of hot organic chemistry in its immediate environment. In addition, they provide independent constraints on the gas temperatures and velocity patterns. The most plausible scenario is that the absorption originates from the inner few AU of the circumstellar disk, perhaps at the footpoint of a disk wind. Further work, both observationally and theoretically, is required to prove this, including a determination of the velocity of IRS 46 itself and monitoring of the infrared lines at high spectral resolution to check for time variability of the radial velocity and/or absorbing column along the line of sight. This detection offers prospects for future high spectral and spatial resolution mid-infrared and submillimeter searches for these and other organic molecules in emission in more face-on disks.

We are grateful to J. Carr and J. Najita for useful discussions and to R. Tilanus for carrying out the JCMT observations. Astrochemistry in Leiden is supported by a Spinoza grant from NWO. Support for this work, part of the Spitzer Legacy Science Program, was provided by NASA through contracts 1224608, 1230779, and 1256316 issued by the Jet Propulsion Laboratory, California Institute of Technology, under NASA contract 1407.

REFERENCES

- André, P., & Montmerle, T. 1994, *ApJ*, 420, 837
 Blake, G.A., & Boogert, A.C.A. 2004, *ApJ*, 606, L73
 Bontemps, S., et al. 2001, *A&A*, 372, 173
 Boonman, A.M.S., van Dishoeck, E.F., Lahuis, F., & Doty, S.D. 2003, *A&A*, 399, 1063
 Brittain, S.D., Rettig, T.W., Simon, T., Kulesa, C., DiSanti, M.A., & Dello Russo, N. 2003, *ApJ*, 588, 535
 Carr, J.S., Evans, N.J., Lacy, J.H., & Zhou, S. 1995, *ApJ*, 450, 667
 Carr, J.S., Tokunaga, A.T., & Najita, J. 2004, *ApJ*, 603, 213
 de Geus, E.J., de Zeeuw, P.T., & Lub, J. 1989, *A&A*, 216, 44
 Doppmann, G.W., Greene, T.P., Covey, K.R., & Lada, C.J. 2005, *AJ*, 130, 1145
 Doty, S.D., van Dishoeck, E.F., van der Tak, F.F.S., & Boonman, A.M.S. 2002, *A&A*, 389, 446
 Draine, B.T. 2003, *ARA&A*, 41, 241
 Dullemond, C.P., & Dominik, C. 2004, *A&A*, 417, 159
 Dutrey, A., Guilloteau, S., & Guélin, M. 1997, *A&A*, 317, L55
 Ehrenfreund, P., & Charnley, S.B. 2000, *ARA&A*, 38, 427
 Eisloffel, J., Mundt, R., Ray, T.P., & Rodríguez, L.F. 2000, in *Protostars & Planets IV* (Tucson: University of Arizona), 815
 Evans, N.J., et al. 2003, *PASP*, 115, 965
 Gail, H.-P. 2002, *A&A*, 390, 253
 Glassgold, A.E., Najita, J., & Igea, J. 2004, *ApJ*, 615, 972
 Gorti, U., & Hollenbach, D. 2004, *ApJ*, 613, 424
 Greaves, J.S. 2005, *Science*, 307, 68
 Ilgner, M., Henning, Th., Markwick, A.J., & Millar, T.J. 2004, *A&A*, 415, 643
 Imanishi, K., Koyama, K., & Tsuboi, Y. 2001, *ApJ*, 557, 747
 Jørgensen, J.K., Schöier, F.L., & van Dishoeck, E.F. 2002, *A&A*, 389, 908
 Kastner, J.H., Zuckerman, B., Weintraub, D.A., & T. Forveille, T. 1997, *Science*, 277, Issue 5322, 67
 Kessler-Silacci, J.E., et al. 2005, *ApJ*, in press; astro-ph/0511092
 Lahuis, F., & van Dishoeck, E.F. 2000, *A&A*, 355, 699
 Markwick, A.J., Ilgner, M., Millar, T.J., & Henning, Th. 2002, *A&A*, 385, 632
 Markwick, A.J., & Charnley, S.B. 2004, *ASSL* 305, *Astrobiology: Future Perspectives*, ed. P.Ehrenfreund et al. (Dordrecht: Kluwer), 33
 Najita, J., Carr, J.S., & Mathieu, R.D. 2003, *ApJ*, 589, 931
 Pontoppidan, K.M., et al. 2003, *A&A*, 408, 981
 Pontoppidan, K.M., Dullemond, C.P., van Dishoeck, E.F., Blake, G.A., Boogert, A.C.A., Evans, N.J., Kessler-Silacci, J.E., & Lahuis, F. 2005, *ApJ*, 622, 463
 Prinn, R.G. 1993, in *Protostars & Planets III* (Tucson: University of Arizona), eds. J.H. Levy & J.I. Lunine, 1005
 Qi, C., Kessler, J.E., Koerner, D.W., Sargent, A.I., & Blake, G.A. 2003, *ApJ*, 597, 986
 Ridge, N.A., et al. 2006, *AJ*, submitted
 Rodgers, S.D., & Charnley, S.B. 2003, *ApJ*, 585, 355
 Thi, W.-F., van Zadelhoff, G.-J., & van Dishoeck, E.F. 2004, *A&A*, 425, 955